THE PENNSYLVANIA STATE UNIVERSITY
SCHREYER HONORS COLLEGE

DEPARTMENT OF CHEMICAL ENGINEERING

# THE EFFECT OF MATRIX RIGIDITY ON HISTONE MODIFICATIONS DURING EPITHELIAL TO MESENCHYMAL TRANSITION

PAUL BLANCHARD
SPRING 2018

A thesis
submitted in partial fulfillment
of the requirements
for a baccalaureate degree
in Chemical Engineering
with honors in Chemical Engineering

Reviewed and approved* by the following:

Esther Gomez
Assistant Professor of Chemical Engineering
Thesis Supervisor

Darrell Velegol
Distinguished Professor of Chemical Engineering
Honors Adviser

* Signatures are on file in the Schreyer Honors College.

## ABSTRACT

Epithelial to mesenchymal transition (EMT) is a process in which an epithelial cell loses its cell-cell adhesion and polarity, and instead gains mesenchymal traits, such as mobility. The human body uses EMT to produce myofibroblasts, which aid in wound healing. However, aberrant activation of EMT to produce myofibroblasts can contribute to fibrosis and cancer progression. One of the pathways that can initiate EMT is through Transforming Growth Factor (TGF)-β1, the effect of which has been shown to change with matrix rigidity. TGFβ1 will induce EMT in cells grown on stiff matrices, but not when grown on soft matrices. The purpose of this research was to determine why this stiffness regulation might occur by determining the role histone modifications play. Histone modifications are chemical modifications that occur on histones, proteins that wrap DNA into chromatin, which regulate what genes are expressed.

Levels of one specific marker, the trimethylation of lysine 36 on histone H3 (H3K36Me3) were shown to increase with increasing rigidity after TGFβ1 treatment, suggesting that it may be involved in the matrix stiffness regulation EMT. Treatment with cell contractility inhibitors resulted in a decrease in the aforementioned histone marks in cells cultured on the stiff gels, which may indicate that increased cell contractility contributes to the way that stiffness regulates histone modifications during EMT. Initial studies of JMJD2A, a demethylase protein which removes a methyl group from histones, indicate that JMJD2A levels increase with increasing rigidity and TGF-β1 treatment. Furthermore, inhibition of demethylases results in a decrease in the expression of the mesenchymal marker alpha smooth muscle actin (aSMA), suggesting that demethylases play an important role in regulating EMT. Additional studies are needed to confirm mechanistically how JMJD2A and the histone mark H3K36Me3 contribute to EMT.

# TABLE OF CONTENTS

## LIST OF FIGURES

# LIST OF TABLES

# ACKNOWLEDGMENTS

I would like to thank Dr. Esther Gomez for allowing me to join her research laboratory and for providing guidance and mentorship throughout the three years I have been involved in her laboratory. Dr. Gomez had provided me the necessary background knowledge and research techniques, supplied me with the necessary equipment, materials, and laboratory space, and helped me determine the necessary experiments. I am grateful that she has taken the time and energy to meet with me many times throughout the semester and provide guidance whenever I have needed it.

I would also like to thank Dr. Joseph O'Connor for his help with learning laboratory and analysis techniques. His willingness to help me through many of my early research problems was critical in me developing the skills needed to complete this thesis. I would further like to thank Tina Lai and Virginia Sanabria for teaching me protein quantification and western blotting imaging respectively, and to all the members of the Esther Gomez Group, for providing assistance when needed and for making my time in lab enjoyable.

I would also like to thank Dr. Wayne Curtis, and Dr. Thomas Wood, for allowing me to use their equipment for protein quantification and western blot imaging. I would also like to thank the Pennsylvania State University Department of Chemical Engineering for providing a summer biofellowship to fund some of this research in both the 2015 and 2017 summers.

I would also like to thank my honors advisor, Dr. Darrell Velegol, for answering all of my questions and for providing assistance with editing my thesis and reaching my career goals. Finally, I would like to thank my friends and family for their constant support throughout my time at Penn State.

# Chapter 1

## Introduction

The objective of this research was to study the role histone modifications play in the matrix stiffness regulation of the epithelial to mesenchymal transition, with applications to myofibroblasts. The paper will explore the role cell contractility and histone demethylase proteins play in the process, and we hypothesize that matrix stiffness will control the levels of histone modifications, and that these modifications will play a role in regulating the initiation of the epithelial to mesenchymal transition.

## Myofibroblasts

Myofibroblasts are differentiated cells that aid the body in wound healing. After an injury, myofibroblasts are created and activated by a series of biochemical and mechanical signals from a variety of precursor cells.[1] One key feature of myofibroblasts is the presence of alpha smooth muscle actin (αSMA), a cytoskeletal protein that is incorporated into stress fibers.[2,3] The inclusion of αSMA increases the contractility of these cells, allowing them to exert large forces on surrounding tissue.[1,2] These large contractile forces, and the extracellular matrix (ECM) proteins that myofibroblasts secrete provides stability to wounded tissue, and assist in wound closure.[2] After the wound is healed, these cells undergo apoptosis to avoid excessive ECM buildup.[3]

However, aberrant or prolonged activation of myofibroblasts can result in organ fibrosis and cancer progression.[4] In fibrosis, myofibroblasts persist, excrete excessive levels of ECM compounds, especially collagen, and continue to exert large forces, which together results in stiffening of tissue and loss of tissue structure.[1,4] Myofibroblasts are also found at the invasive

fronts of metastatic cancer, and have been shown to be linked with cancer progression and metastasis.[1,4,5] These cells make up part of the tumor-associated stroma, and have been identified as one of the most important components of the stroma in influencing tumor progression and metastasis.[5] Myofibroblasts produce extracellular matrix proteases, lymphogenic factors, and chemokines, such as vascular endothelial growth factor, which organize the tumor microenvironment and can promote metastasis.[1,5]

Myofibroblasts are formed from a variety of different cells in different parts of the body, however, studies have shown that epithelial to mesenchymal transition (EMT) is a major pathway for myofibroblast formation.[1,6,7] In renal fibrosis, studies have estimated that more than a third of disease-related fibroblasts originated from nearby epithelial cells.[6] EMT also plays a role in many important developmental processes, especially in embryonic development.[7,8]

## Epithelial to Mesenchymal Transition

Epithelial cells are characterized by polarity and tight cell-cell contact.[6,8] These cells serve as protective monolayer barriers between systems of an organism, and are bound together by tight junctions, adheren junctions, and gap junctions.[1,7,8] During EMT, cells lose these epithelial traits, and gain mesenchymal traits such as increased mobility, cytoskeleton remodeling, elongation, a lack of cell-cell adhesion, and increased actin stress fiber levels.[1,3,8]

EMT is initiated by many different signaling pathways, including the Transforming Growth Factor Beta (TGFβ1), Wnt, and Notch signaling pathways.[1,6,9] These pathways, along with many other factors, work together to induce EMT. In many cases, different factors can be involved in the induction of EMT for different tissues.[8] One of most common and well characterized inducers of EMT is TGFβ1, a protein that promotes the loss of cell-cell contact and

polarity and the gain of contractility and mobility.[4] TGFβ1 works by binding to serine-threonine receptors on a cell surface, and forming a dimeric receptor complex, which phosphorylates and activates Smad transcription factors.[1,6,9] Activated transcription factors translocate to the nucleus and change gene expression.[1,6,9] In addition to the Smad pathway, TGFβ1 also activates several other pathways, including p38 mitogen-activated protein kinase (p38MAPK), focal adhesion kinase (FAK), phosphoinositide 3-kinase (PI3K)-Akt, RhoA, and extracellular signal-regulated kinase (ERK), which regulate cytoskeletal organization, stress fiber formation, and upregulation of many mesenchymal genes.[7,9] These pathways activate many other transcription factors such as Snail, Slug, ZEB, and bHLH transcription factors.[6] In many cases, the genes activated by these factors will upregulate proteins involved in the induction of EMT, so feedback loops can be created to maintain cells as mesenchymal.[8]

As a result of these transcription factors, cells experience downregulation of epithelial markers, such as E-cadherin, syndecan-1 and zona occludens (ZO)-1, and upregulation of mesenchymal markers, such as N-cadherin, caldesmon, vimentin and αSMA.[6,9,10] A major change that occurs is downregulation of epithelial filament proteins and upregulation of mesenchymal intermediate filament proteins.[9] In epithelial cells, keratin proteins make up the majority of intermediate filaments, and promote cell-cell adhesion, however, during EMT, keratin proteins are downregulated, and vimentin, a mesenchymal intermediate filament structural protein, is overexpressed. In addition, changes in other cytoskeletal proteins including tropomyosin and caldesmon, results in an increase in the number, width, and length of actin filaments.

## EMT and Tissue Stiffness

Extracellular matrix stiffness plays a role in regulating cellular processes, including differentiation and proliferation, and has been shown to play a large role in regulating the induction of EMT.[4] During breast tumor progression for instance, the Young's modulus of the mammary gland increases from 300 Pa to over 5000 Pa.[11, 12] In addition, increased matrix rigidity has been linked to increased EMT, myofibroblast activation, and harmful contractile activity. Extracellular stiffness can affect cells by regulating the cytoskeletal architecture, which can increase cell contractility and integrin engagement. Together, these effects promote increased activation of latent TGFβ1, and promote the initiation of EMT. Recent studies have shown that extracellular rigidity is crucial in regulating TGFβ1 initiated EMT.[1] TGFβ1 will initiate EMT in cells grown on stiff substrata but will not initiate EMT on soft substrata.[1,4]

Various studies have tried to explain the matrix stiffness regulation of EMT, and several EMT signaling pathways and transcriptional factors have been linked to stiffness. The PI3K/Akt signaling pathway has been shown to be linked to matrix stiffness, as increased matrix stiffness is associated with increased phosphorylation of Akt, and therefore increased activation of the pathway.[13] In addition, the subcellular localization of myocardin related transcription factor (MRTF)-A, is associated with TGFβ-regulated EMT, and has been shown to be controlled by the organization of the actin cytoskeleton, with an increase in nuclear localization with increased matrix rigidity.[4,9] This research aims to further explain how rigidity regulates EMT by studying how tissue stiffness controls histone modifications during EMT initiation.

## Histone Modifications

In order for transcriptional factors to up or down regulate genes, histone modifications need to occur. Histone are proteins in the nucleus of eukaryotic cells, that tightly pack DNA into nucleosome units which are further folded into chromatin.[14] In order for a gene to be transcribed, chromatin needs to be locally unwound by histone proteins in order for transcriptional factors to access DNA. Post-translational modifications to these histones, such as acetylation, methylation or phosphorylation, regulate gene transcription by controlling chromatin packing.[14] A wide range of modifications have been associated with either gene repression or gene activation, and several have been linked to epithelial to mesenchymal transition.

Several studies have shown that histone modification has been linked to EMT initiation, and one of the most studied links is the activation of the Snail-1 zinc finger transcription factor, which represses E-cadherin, an epithelial marker.[15] E-cadherin maintains epithelial characteristics and promotes cell-cell junctions, however, Snail-1 directly represses the transcription of E-cadherin. Snail-1 has been shown to recruit LSD1 histone demethylase to E-cadherin promoters, which demethylates dimethylated lysine 4 on histone 3 (H3K4Me2).[16,17,18] Epithelial cells have been shown to have relatively high levels of H3K4Me2 at the E-cadherin gene promoter, and a decreased level has been linked to decreased E-cadherin level and EMT initiation.[15,16,18] Decreased levels of acetylation on lysine 4 on histone 3 (H3K4Ac) and increased levels of H3K27Me3 have also been linked to decreased E-cadherin levels.[16]

Histone modifications have also been linked to some of the pathways by which matrix stiffness has been shown to regulate EMT, such as the nuclear localization of MRTF-A. Studies have shown that methylation of lysine 4 on histone 3 is required for some of the MRTF-A mediated gene upregulation necessary for EMT and cell migration to occur.[17] Further studies

have shown that this methylation is performed by a methyltransferase known as SMYD3.[17] Since histone modifications and stiffness are both linked to this mechanism involved in EMT, we expect histone modifications to be responsible in part for other aspects of the matrix rigidity regulation of EMT.

One modification in particular is being studied in this report, the trimethylation of lysine 36 on histone H3 (H3K36Me3). This mark is typically found near the promoter region of genes, and bulk levels of H3K36Me3 have been shown to increase after TGFβ treatment, possibly as the result of the lysine-specific demethylase-1 (Lsd1).[19] These increased levels of H3K36Me3 are typically found in gene rich regions with EMT related functions.[20] Little research, however, has been conducted related to how H3K36Me3 levels are controlled by matrix rigidity. As shown in Figure 1, levels of H3K36Me3 are primarily controlled by the interaction between JMJD2A, a demethylase protein, which demethylates H3K36Me3 and SETD2, a methyltransferase protein, which adds a methyl group to H3K36Me2.

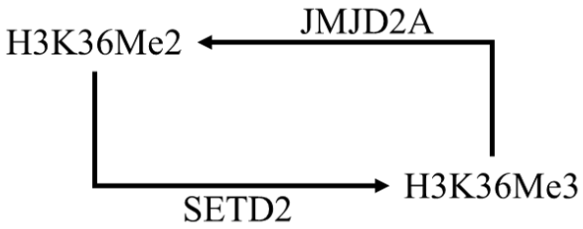


**Figure 1. Conversion between H3K36Me3 and H3K36Me2**

## Purpose of the Study

In this thesis, the role histone modifications play in the extracellular matrix stiffness mediated regulation of EMT was studied. The primary focus was studying H3K36Me3, however, acetylation on histone 4 was also studied. Normal Murine (Mouse) Mammary Gland (NMuMG) epithelial cells were grown on polyacrylamide gels of varying stiffness, and levels of histone

markers were studied across stiffness levels and with and without TGFβ1, an inducer of EMT to determine if histone modification levels varied with stiffness. We hypothesized that matrix stiffness will regulate the effect of TGFβ1 and will control the levels of TGFβ1-mediated histone modifications. Additionally, the effects of Y-27632 and Blebbistatin, two contractility inhibitors, were tested on histone marker levels, to determine if cell contractility regulates histone modification levels. Finally, levels of JMJD2A, a protein that demethylates a histone, were compared across rigidity, and a JMJD2A inhibitor was tested to determine its effect on EMT.

# Chapter 2

## Procedure

### Solution Preparation

Prior to experimentation, the required solutions were prepared based on the following specifications. 1× Phosphate Buffered Saline (PBS) was prepared by diluting 10 × PBS with deionized water ($dH_2O$). 4-(20hydroxyethyl)-1-piperazineethanesulonic acid (HEPES solution) was diluted to 50 mM by adding $dH_2O$, and sodium hydroxide was added until a pH of 8.5 was reached. 1 × Tris Buffer Saline with tween (TBST) buffer was prepared by diluting 10 × TBS in $dH_2O$ and adding 0.1% tween.

### Polyacrylamide Gel Preparation

Polyacrylamide gels, polymer gels with tunable stiffness, were prepared to serve as substrates for cell growth, and to study the effects of stiffness. 22-mm square glass slides were incubated in 0.1 M NaOH for 15 minutes and washed with $dH_2O$. Slides were then incubated for 30 minutes in a 2% (v/v) 3-aminopropyltrimethoxysilane (APTMS) in acetone solution and rinsed with acetone. Next, slides were incubated in 0.5% glutaraldehyde diluted in 1× PBS and washed with $dH_2O$. Additionally, 22-mm diameter circular slides were coated in Rain-X.

Polyacrylamide (PA) gels were prepared at the following stiffness: 300 Pa, 900 Pa, 2000 Pa, 4000 Pa, 6300 Pa by mixing a 40% acrylamide (A) solution, a 2% N, N'-methylene bisacrylamide (B), and $dH_2O$ at the levels shown in Table 1 and degassing for 30 minutes.

**Table 1. Polyacrylamide Gel Stiffness and Composition**

| Stiffness (Pa) | Percent A | Percent B | Volume A (µL) | Volume B (µL) | Volume Water (µL) |
|---|---|---|---|---|---|
| 300 | 5% | 0.015% | 125 | 7.5 | 862 |
| 900 | 5% | 0.03% | 125 | 15 | 854.5 |
| 2000 | 5% | 0.06% | 125 | 30 | 839.5 |
| 4000 | 5% | 0.35% | 125 | 175 | 694.5 |
| 6300 | 7.5% | 0.2% | 187.5 | 100 | 707 |

0.5 µL of N, N, N', N'-tetramethylethylenediamine (TEMED) and a 5 µL of a 10% solution of ammonium persulfate (APS) in $dH_2O$ were added to each acrylamide to initiate polymerization. Immediately after, 20 µL of the solution was placed in the center of each 22-mm slide, which was covered with a Rain-X treated circular slide. Gels were allowed to polymerize for 30 minutes, after which glass slides and gels were placed in 1×PBS and stored in a 4 °C refrigerator until activation.

## Activation of Polyacrylamide Gels

In order for cells to attach to polyacrylamide gels, the surface of the gels needed to be functionalized with fibronectin. To do this, sulfosuccinimidyl 6-(4'-azido-2'-nitrophenylamino) hexanoate) (Sulfo-SANPAH) was dissolved in HEPES solution to make a 0.5 mM solution. The circular glass cover slide was removed from the gels, 200 µL of sulfo-SANPAH solution was pipetted on top of each gel, and the gels were placed in the CL-1000 Ultraviolet Crosslinker for 10 minutes. Remaining sulfo-SANPAH solution was aspirated off of the gels, and HEPES was used to wash off any remaining sulfo-SANPAH. An additional 200 µL of sulfo-SANPAH was placed on each gel, and the gels were again placed in the ultraviolet crosslinker for 10 minutes.

Gels were taken to the cell-culture hood, and rinsed three times with sterile HEPES. A solution of 0.1 mg/ml human fibronectin diluted in HEPES was added on top of the gels and allowed to incubate for 2 hours. Excess fibronectin solution was removed with a 1 × PBS washing, and gels were incubated in 70% ethanol for 30 minutes, and exposed to UV light for 15 minutes, before again being washed with 1 × PBS.

## Coating Glass Coverslips with Fibronectin

22-mm square glass slides were sterilized by incubating with 70% ethanol for 30 minutes, and exposing to UV light for 15 minutes. The slides were washed with 1× PBS and covered with 0.1 mg/ml human fibronectin diluted in HEPES for 2 hours. Extra fibronectin was removed by washing with 1× PBS.

## Cell Culture

Normal murine mammary gland epithelial (NMuMG) cells (American Type Culture Collection) were cultured in a media consisting of Dulbecco's Modified Eagle Medium (DMEM), 10 μg/ml insulin, 50 μg/ml gentamicin, and 10% fetal bovine serum (FBS). Gels were seeded at 150,000 cells per 22-mm diameter gel, and glass slides were seeded at 50,000 cells per slide. 24 hours after seeding, cells were treated with 10 nM recombinant human transforming growth factor TGFβ1 to induce epithelial to mesenchymal transition, or a control solution made of the TGFβ1 solvent (1 % bovine serum albumin (BSA) in 4 mM HCl) for 48 hours. The following inhibitors were diluted in dimethyl sulfoxide (DMSO) and were used for experiments: 450 nM JIB-04, 0.01 nM Blebbistatin, or 0.01 nM Y-27632.

## Immunofluorescence

Immunofluorescence was used to visualize and quantify protein expression. For staining of αSMA, cells were fixed at -20 °C with a solution of 1:1 methanol/acetone for 10 minutes. For all other staining, cells were fixed with 4% paraformaldehyde (PF) for 15 minutes at room temperature. Samples were rinsed with 1× PBS and samples fixed with PF were treated with 0.5% IGEPAL twice for 10 minutes and 0.1 % Triton X-100 for 10 minutes to permeabilize the cells. After cells were fixed, samples were treated with their respective blocking buffer for 1 hour. Blocking buffers for different antibodies are shown in Table 2.

**Table 2. Blocking Buffers for Primary Antibodies**

| Primary Antibody | Blocking Buffer Composition |
|---|---|
| H3K36Me3 | 0.3% Triton – X, 5% goat serum, 1% BSA |
| aH4 | 0.1% Triton – X, 10% goat serum |
| JMJD2A | 0.1% Triton – X, 10% goat serum, 1% BSA |
| αSMA | 0.5% Tween, 10% goat serum, |

After, samples were incubated with the following primary antibodies: H3K36Me3 (Cell Signaling Technology, Product Number 9763), acetylated Histone H4 (aH4) (Millipore, Catalog Number: 05-1355), αSMA (Sigma-Aldrich, Lot Number: 129K4819), and JMJD2A (ThermoFisher Scientific, Catalog Number: MA5-14782). H3K36Me3 was incubated at a 1:100 dilution overnight, aH4 was incubated at a 1:500 dilution for 1 hour, αSMA was incubated at a 1:200 dilution for 1 hour, and JMJD2A was incubated at a 1:200 dilution overnight. Samples were washed with 1× PBS to remove unbound primary antibody, and incubated in Alexa Fluor-conjugated secondary antibody for one hour at 1:500 dilution, and again washed three times with

1× PBS. Cell nuclei were counterstained with Hoechst 33342 (Invitrogen). After staining, samples were mounted to glass slides using Fluoromont-G.

Samples were imaged using a 20 × objective on a Nikon Eclipse Ti-E inverted fluorescence microscope with a Photometrics CoolSNAP $HQ^2$ CCD camera. Relative protein expression levels were calculated using ImageJ software. For αSMA expression, a cut-off level of expression was chosen, and the fraction of cells that expressed the protein were compared. All experiments were performed a minimum of three times, and statistical analysis was performed using analysis of variance (ANOVA) followed by the Bonferroni post – hoc correction using Kaleidagraph v2.4 software. Data was judged significant when the p value was less than 0.05. Data was normalized for each trial relative to the 300 Pa, control treated sample, and the mean of the trials with the standard error between the means of each individual trial were reported.

## Protein Extraction and Quantification

Cells were plated at 750,000 cells per 10-cm tissue culture dish and cultured in the same media conditions as before. Cells were treated with or without TGFβ1 and inhibitors 12 hours after plating in the same concentrations described earlier. After 48 hours, cells were washed two times with ice-cold 1× PBS, and were covered with 1 mL of RIPA lysis buffer containing 1% Halt phosphatase/protease inhibitor and 1% EDTA for 30 minutes. Cells and the remaining fluid was scraped off of dish, and centrifuged at 12000 g for 10 minutes at 4 $^{\circ}$C. The protein solution was collected and stored at -80 $^{\circ}$C.

Protein concentration was quantified using a Pierce BCA Protein Assay Kit (Thermo Scientific). Nine standard concentrations of bovine serum albumin (BSA) diluted in RIPA buffer

and the protein samples were loaded in a 96 well plate, and working reagent of 50:1 Pierce BCA assay reagent A to reagent B was added to each diluted protein. The samples were incubated at 37 °C for 30 minutes, and absorbance was measured using a Spectramax Plus 384 micro plate reader and Magellan Tecan Sunrise software at 582 nm. A standard protein concentration curve was made and the concentration of protein samples was determined based on comparison to the standard curve.

## Western Blotting

Western blotting was used to quantify protein levels and compare these levels across protein samples. Each protein sample prepared via protein extraction discussed earlier with 25 percent NuPAGE LDS sample buffer (4×) and 10 percent NuPAGE reducing agent (10×) was heated at 70 °C for 10 minutes to denature samples. After, the protein sample was electrophoresed on a NuPAGE 4-12% Bis-Tris Gel for approximately 50 minutes at 200 V using NuPAGE MOPS SDS Running Buffer in a XCell SureLock Electrophoresis Cell powered by a Bio-Rad PowerPac HC. After electrophoresis, an Invitrolon PVDF transfer paper was incubated for 30 seconds in pure methanol, and then the transfer paper, extra-thick blot paper, and the gel were soaked with 2× NuPAGE Transfer Buffer (10% NuPAGE Transfer Buffer (20×), 0.1% NuPAGE Antioxidant, 0.03% SDS in $dH_2O$). The soaked extra-thick blot paper was placed inside a Bio-Rad Trans-Blot SD Semi-Dry Transfer Cell, and the transfer paper, gel, and second piece of blot paper were laid on top. The transfer was run at 15 V for 30 minutes. Transfer paper was incubated in Ponceau S for 5 minutes, and washed with TBST buffer to visualize protein transfer to the membrane. Paper was incubated for one hour in a blocking buffer

comprised of 1% BSA, and 0.1% tween in TBST buffer, and incubated overnight in a 1:1000 dilution of JMJD2A primary antibody (ThermoFisher Scientific, Catalog Number: MA5-14782) in blocking buffer. Transfer paper was washed three times with TBST buffer, treated with a horseradish peroxidase (HRP)-linked secondary antibody for one hour, and again washed three times with TBST buffer. Each sample was incubated in a 50:50 mixture of Pierce SuperSignal West Dura Stable Peroxide buffer and Luminal enhancer solution for 3.5 minutes. Immediately after, a FluorChem FC2 system was used to image each sample. Data was analyzed using ImageJ.

# Chapter 3

## Results and Discussion

### Stiffness and Histone Modifications

Studies have shown that the stiffness of the mammary gland varies from ~300 Pa to ~5000 Pa for normal and cancerous tissue.[11,12] To mimic the stiffness difference and therefore the potential different effects from TGFβ1 treatment in healthy and diseased mammary tissue, polyacrylamide gels were made with stiffnesses spanning the in vivo stiffnesses of mammary tissue. Cells were cultured on the gels to study how the cells respond to the combined effects of TGFβ1 and matrix stiffness.

Levels of acetylation on histone H4 were measured and compared for cells grown on gels of varied stiffness, and with or without TGFβ1 (a potent inducer of EMT) treatment using immunofluorescence staining, as shown in Figure 2.

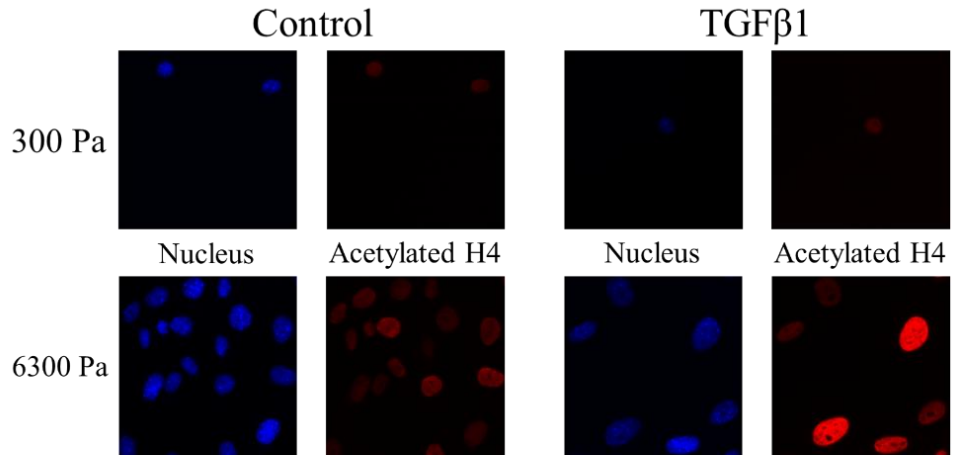


**Figure 2. Nuclear (Blue) and Acetylated H4 (Red) Immunofluorescence Staining of ± TGFβ1 Treated Samples Grown on Gels of Varying Stiffness**

Figure 3 shows relative levels of acetylated H4 that were quantified from microscopy images by computing the integrated intensity of acetylated H4 staining and then normalizing to the control treated cells cultured on 300 Pa substrates.

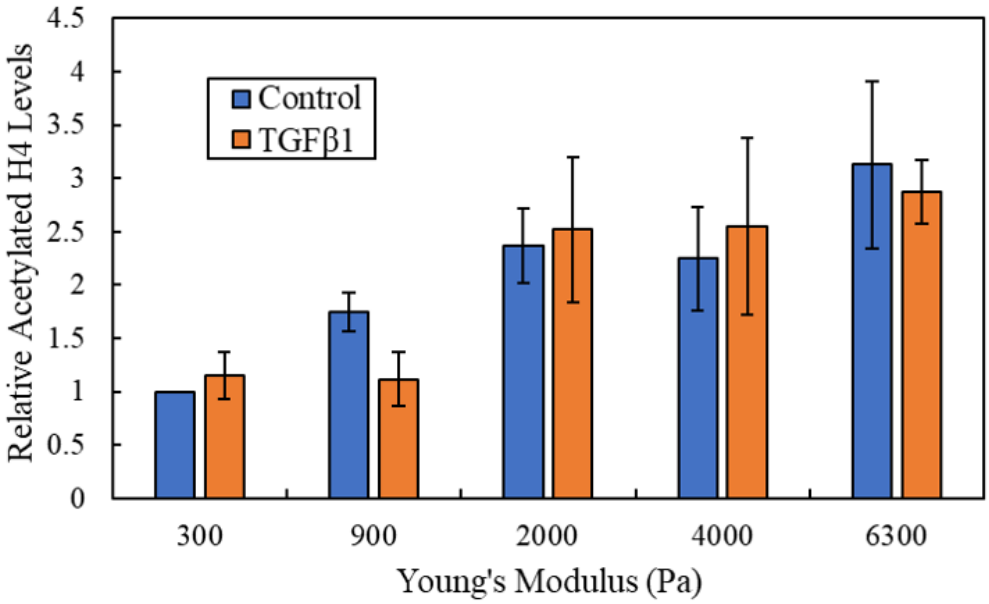


**Figure 3. Relative Acetylated H4 Levels for Cells Grown on Gels of Varying Stiffness with ± TGF-β1 Treatment**

While there appears to be an increase in the levels of acetylation with increasing rigidity, there is no discernable difference between TGFβ1 and control treated samples. Thus, while matrix stiffness may play a role in regulation of the levels of acetylation, TGFβ1 does not appear to play a significant role in the regulation of acetylation of histone H4 during EMT.

Another histone modification, the trimethylation of lysine 36 on histone H3 was also studied to see how it was affected by matrix stiffness and TGFβ1. Cells were stained for the H3K36Me3 mark as shown in Figure 4, and levels of H3K36Me3 were measured as a function of varying stiffness, as shown in Figure 5.

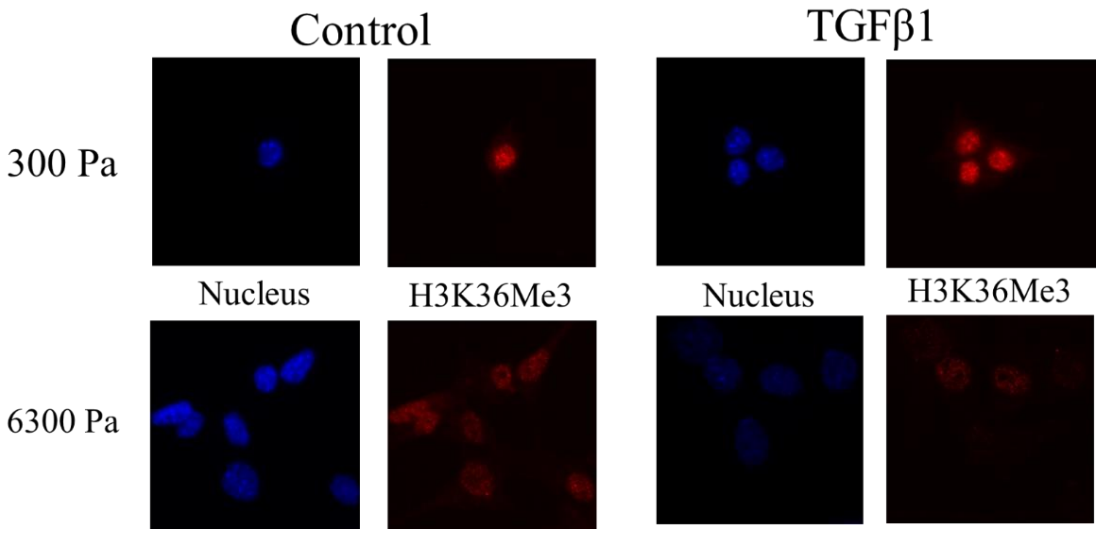


**Figure 4. Nuclear (Blue) and H3K36Me3 (Red) Immunofluorescence Staining of ± TGFβ1 Treated Samples Grown on Gels of Varying Stiffness**

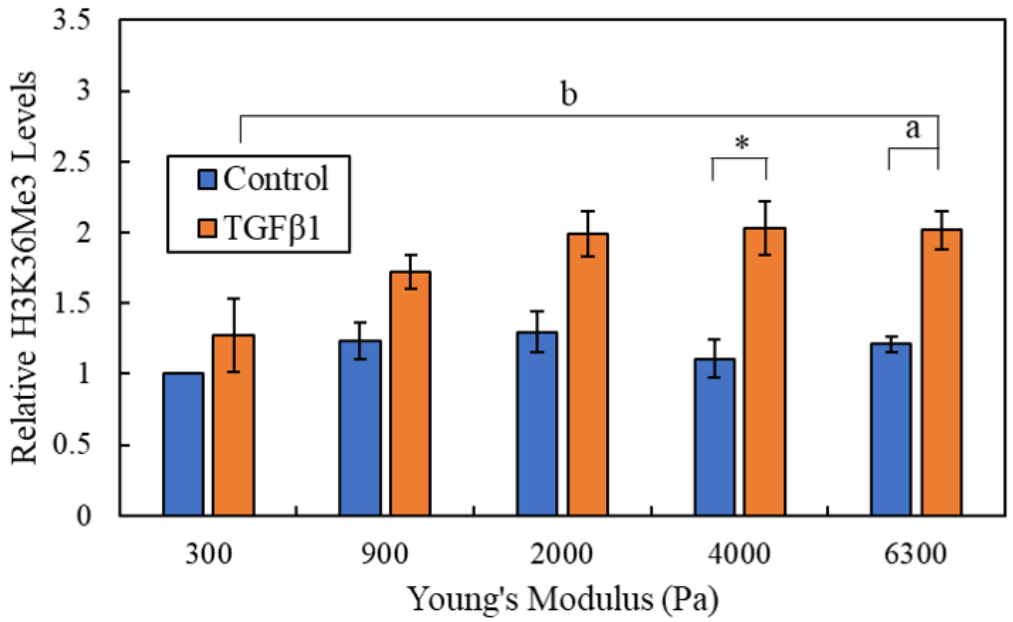


**Figure 5. Relative H3K36Me3 Levels for Cells Grown on Gels of Varying Stiffness with ± TGF-β1 Treatment, *p <0.05, a: p=0.1, b: p=0.16**

Levels of H3K36Me3 increase after TGFβ1 treatment and increase with increasing stiffness at lower stiffnesses after TGFβ1 treatment. Between 300 to 2000 Pa, levels of H3K36Me3 increase with increasing rigidity after TGFβ1 treatment but remain constant with

increasing rigidity at higher stiffness. Levels of H3K36Me3 appear unchanged with increasing rigidity on control treated samples. This suggests that increased levels of H3K36Me3 may play a role in regulating the response of cells to TGFβ1-induced EMT as a function of stiffness. Cells treated with TGFβ1 grown on lower stiffness substrates (300 and 900) will not undergo EMT, while the cells treated with TGFβ1 grown on higher stiffness substrates will undergo EMT.[4] At the levels of stiffness required to undergo EMT, H3K36Me3 levels are raised following treatment with TGFβ1 and are unchanged by stiffness alone. Furthermore, these data suggest that a combination of TGFβ1 treatment and increased matrix stiffness is necessary to induced increased levels of H3K36Me3 within cells.

## Cell Contractility

To determine if increased contractility was the mechanism by which stiffness increases the levels of certain histone modifications in cells, cells were treated with contractility inhibitors. Blebbistatin dissolved in DMSO, an inhibitor that works by directly inhibiting myosin II ATPase and cell contractility and Y27632 dissolved in DMSO, an inhibitor that works by inhibiting Rho/ROCK, which regulate the cytoskeleton and causes cells to make stress fibers, were used to treat cells along with DMSO as a control. As most significant differences occurred between the histone modifications on the softest and stiffest gels, only these gels will be studied in future experiments. Figure 6 shows relative levels of acetylation on histone H4 in cells grown on gels with Young's moduli of 300 and 6300 Pa (corresponding to normal and diseased mammary

tissue stiffness, respectively), with ± TGFβ1 and with the different inhibitors.

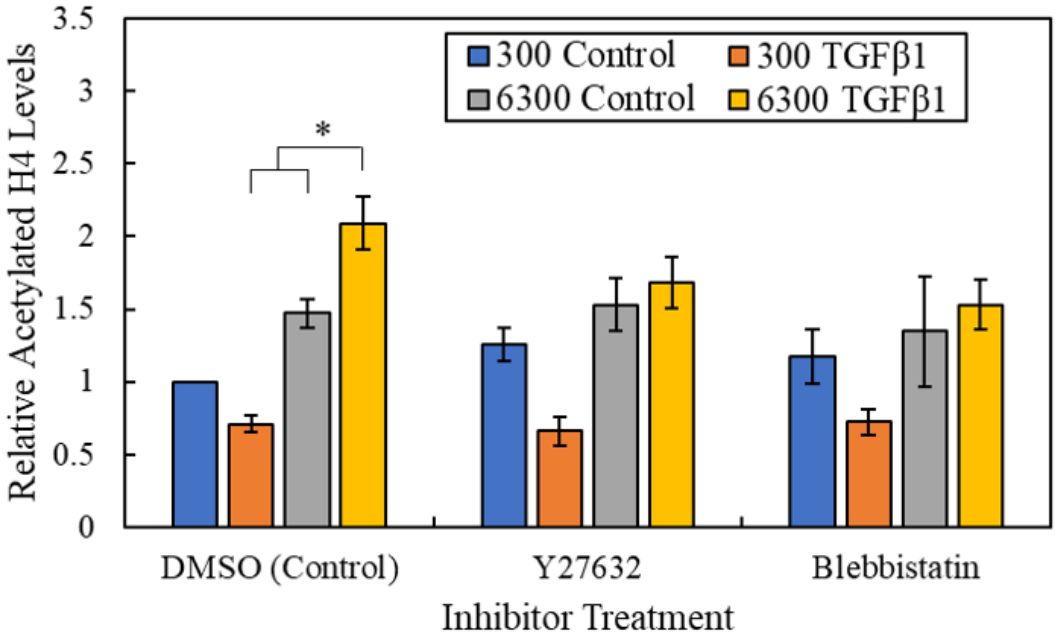


**Figure 6. Relative Acetylated H4 levels for Cells Grown on Gels of Varying Stiffness with ± TGF-β1 Treatment and Inhibitor Treatment, *p <0.05**

Treating with the contractility inhibitors decreases the levels of acetylated histone H4 in the cells cultured of stiffer substrates (6300 Pa) after TGFβ1 treatment (yellow columns in Figure

6) back to the levels of the control treated sample, but differences for the TGFβ1 treated samples between inhibitor treatments were not statistically significant.

Levels of H3K36Me3 were also studied, and Figure 7 shows relative levels of H3K36Me3 in cells grown on gels with Young's moduli of 300 and 6300 Pa with ± TGFβ1 and with the different inhibitors.

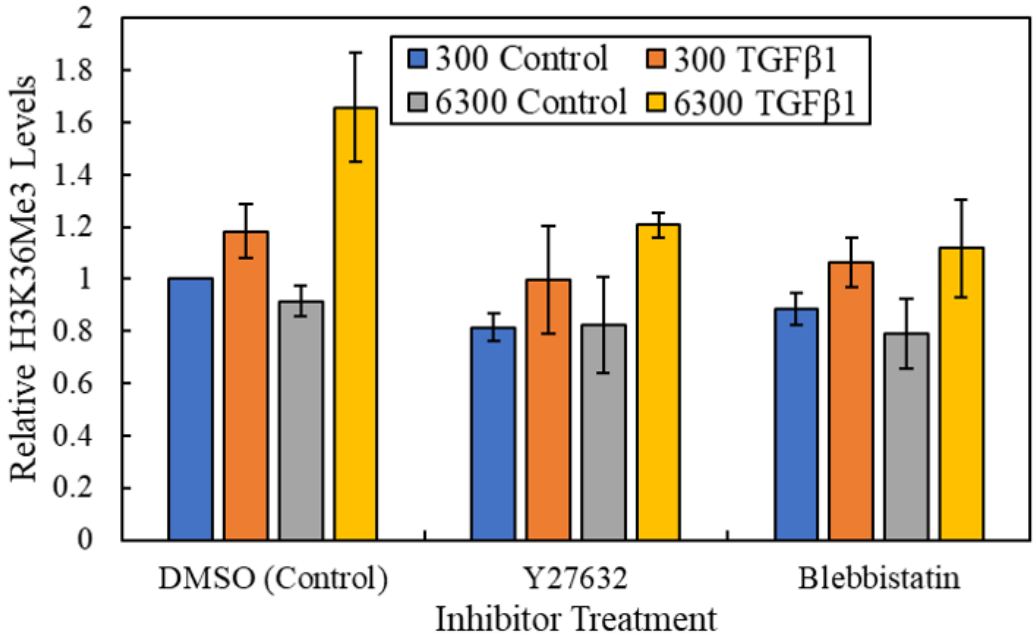


**Figure 7. Relative H3K36Me3 levels for Cells Grown on Gels of Varying Stiffness with ± TGF-β1 Treatment and Inhibitor Treatment**

Similar to the acetylation data, treating with contractility inhibitors appears to decrease the amount of H3K36Me3 in cells grown on stiff gels (6300 Pa) after TGFβ1 treatment, however large standard errors for the DMSO treated sample results in no significance between data points. This data suggests that cell contractility may be a mechanism by which matrix rigidity affects histone modifications after TGFβ1 treatment when cells are cultured on stiff substrates mimicking the mechanical properties of breast tumors, however, no true conclusions can be drawn.

## Histone Demethylase Proteins

Data appears to suggest that cell contractility causes H3K36Me3 levels to increase after TGFβ1 treatment on stiffer gels, which may mean that H3K36Me3 levels are linked to EMT only occurring after TGFβ1 treatment on stiffer gels. The histone modification H3K36Me3 occurs when histone methyltransferases add a methyl group to the dimethylated lysine 36 on histone H3 (H3K36Me2) and is returned to the H3K36Me2 state when a demethylase removes a methyl group from H3K36Me3. One histone demethylase, JMJD2A, a Jumonji domain 2 protein, selectively demethylates lysine 36 and lysine 9 on histone H3. We hypothesized that JMJD2A may regulate H3K36Me3 levels in cells in response to TGFβ1 and substrate stiffness. To test this hypothesis, an immunofluorescence study was done to quantify the amount of JMJD2A in the cells under different culture conditions, shown in Figure 8.

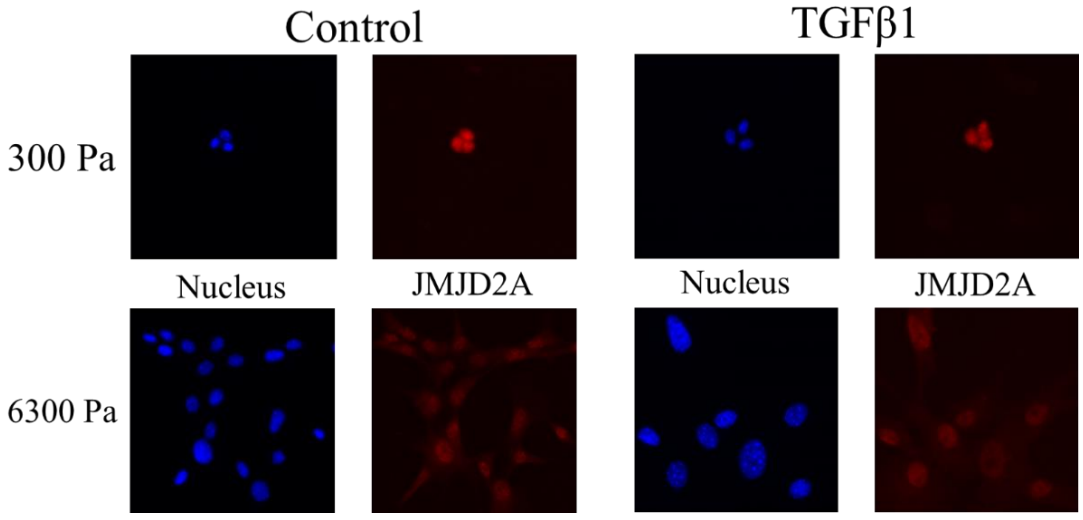


**Figure 8. Nuclear (Blue) and JMJD2A (Red) Immunofluorescence Staining of ± TGFβ1 Treated Samples Grown on Gels of Varying Stiffness**

Figure 9 shows relative JMJD2A levels in the nucleus of cells for cells grown on either soft or stiff gels, treated with either TGFβ1 or a control.

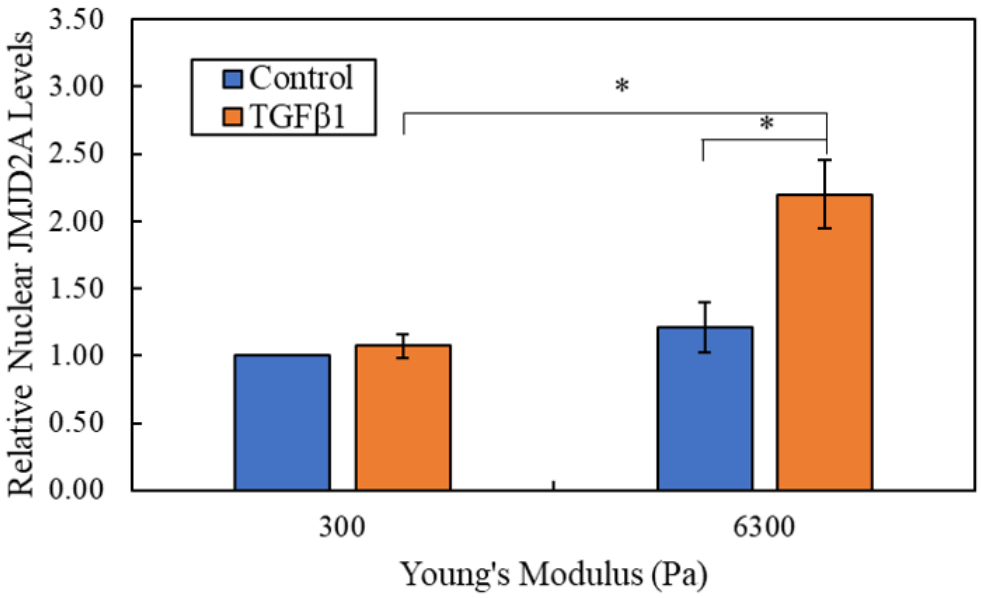


**Figure 9. Relative JMJD2A Levels in the Nucleus for Cells Grown on Gels of Varying Stiffness with ± TGF-β1 Treatment, *p<0.05**

JMJD2A levels in the nucleus increase in cells cultured on stiff substrates after TGFβ1 treatment. This increase in JMJD2A, which removes a methyl group from H3K36Me3 is the opposite of what was expected based on the H3K36Me3 levels trend, in which H3K36Me3 levels increased with increasing rigidity after TGFβ1 treatment. This may indicate that an increase in methyltransferases, proteins that add methyl groups to histones, is occurring in a greater amount than JMJD2A is increasing. Alternatively, even though JMJD2A is localized to the nucleus its activity may be reduced and thus it is not able to demethylate H3K36.

A western blot study of JMJD2A levels was also completed, in which cells were grown on tissue culture dishes, and bulk protein levels within cells were quantified. Levels of JMJD2A

were quantified in Figure 10, and levels of GAPDH, a housekeeping protein that should remain constant for all NMuMG cells, was quantified to normalize JMJD2A levels.

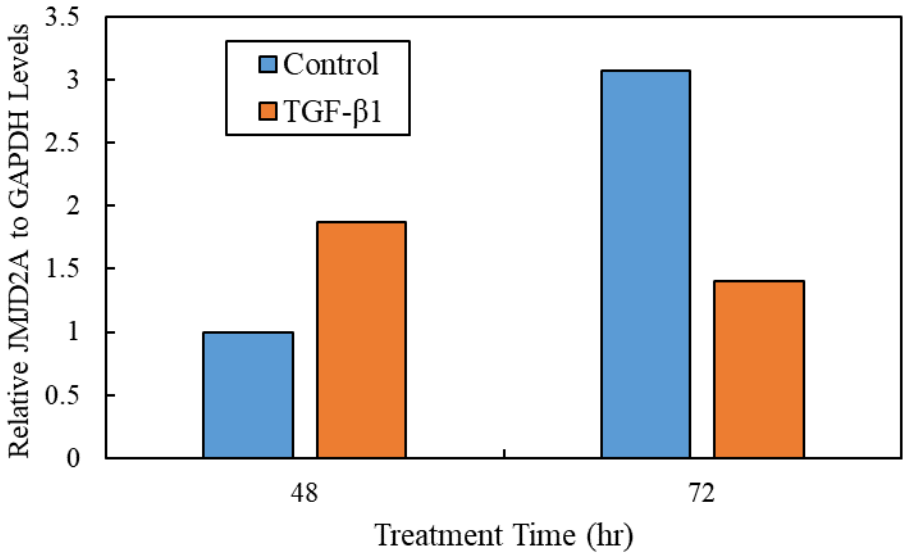


**Figure 10. Relative Levels of JMJD2A Normalized to GAPDH Levels for ± TGF-β1 Treatment and for Different Exposure Times**

Results at 48 hours following treatment with TGFβ1 or control appears to follow the same trend that was seen in the immunofluorescence testing on stiff gels; however, at 72 hours, the opposite trend is seen, where control treated samples have higher JMJD2A levels than the TGFβ1 samples do. More studies will need to be done to confirm and explain these results.

Localization of JMJD2A to the nucleus was also studied and is shown in Figure 11. In order for JMJD2A to demethylate H3K36Me3, it needs to be in the nucleus of the cell. This analysis was done by comparing levels of JMJD2A in the nucleus to levels of JMJD2A in the cytoplasm of the cell. Cells which have significantly higher levels of JMJD2A in the nucleus were considered to have nuclear localization, while cells with significantly higher levels of JMJD2A in the cytoplasm were considered to have cytoplasmic localization. Results showed

higher levels of nuclear localization in cells grown on stiff gels, but localization did not appear to change between control and TGFβ1 samples.

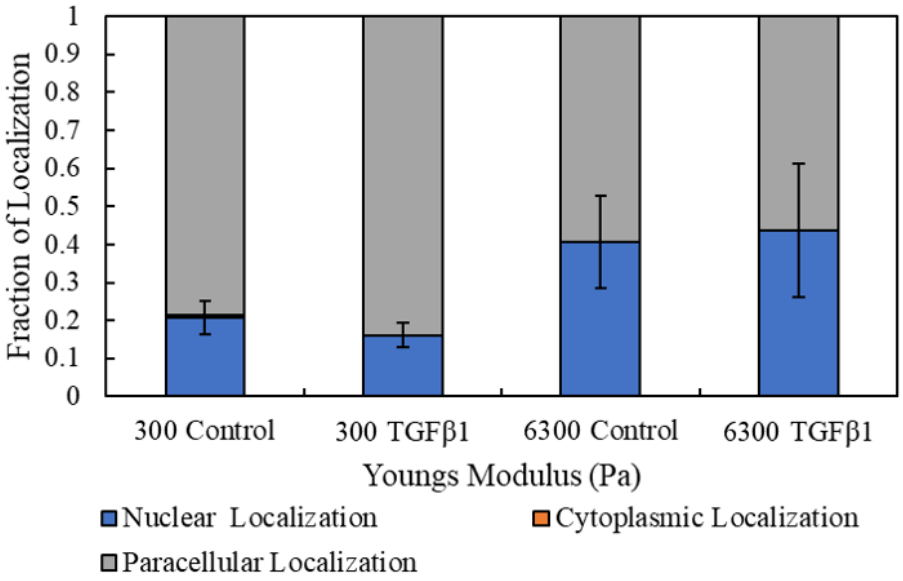


**Figure 11. Fraction of Cells with Nuclear and Cytoplasmic Localization for Gels of Different Stiffness and with ± TGF-β1 Treatment**

The effect of JMJD2A on EMT was also studied, to determine if JMJD2A, played a role in TGFβ1 mediated EMT, by studying an inhibitor, JIB-04, which selectively inhibits JMJD2A. In this experiment, cells on glass slides were treated with either JIB-04 or DMSO as a control, and with TGFβ1 to initiate EMT, or a control. Immunofluorescence staining was performed to visualize αSMA, a mesenchymal marker, and results are shown in Figure 12.

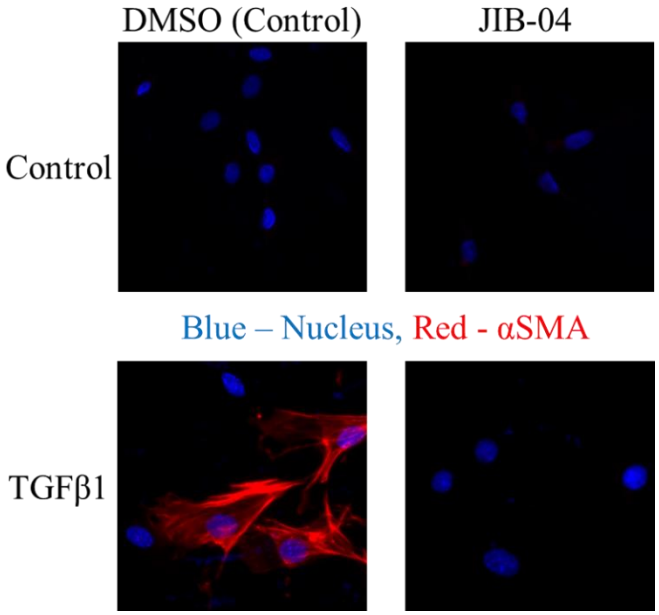


**Figure 12. Nuclear (Blue) and αSMA (Red) Immunofluorescence Staining of ± TGFβ1 and ± JIB-04 (JMJD2A Inhibitor) Treated Samples Grown on Glass Slides**

The fraction of cells expressing αSMA was compared across samples, and results are shown in Figure 13.

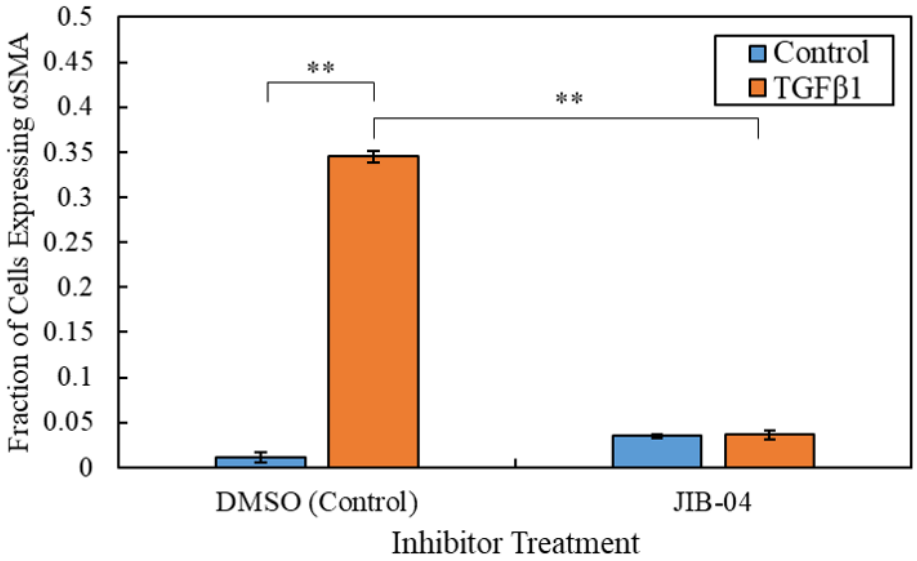


**Figure 13. Fraction of Cells Expressing αSMA for Cells Grown on Glass with ± TGF-β1 Treatment and ± JIB-04 Inhibitor Treatment, **p<0.0001**

Treatment with JIB-04 decreases the fraction of cells that express αSMA, which suggests that JMJD2A may be needed in order for cells to express αSMA and may be important in determining whether or not a cell undergoes EMT. These experiments were repeated on both soft and stiff gels, as shown in Figure 14.

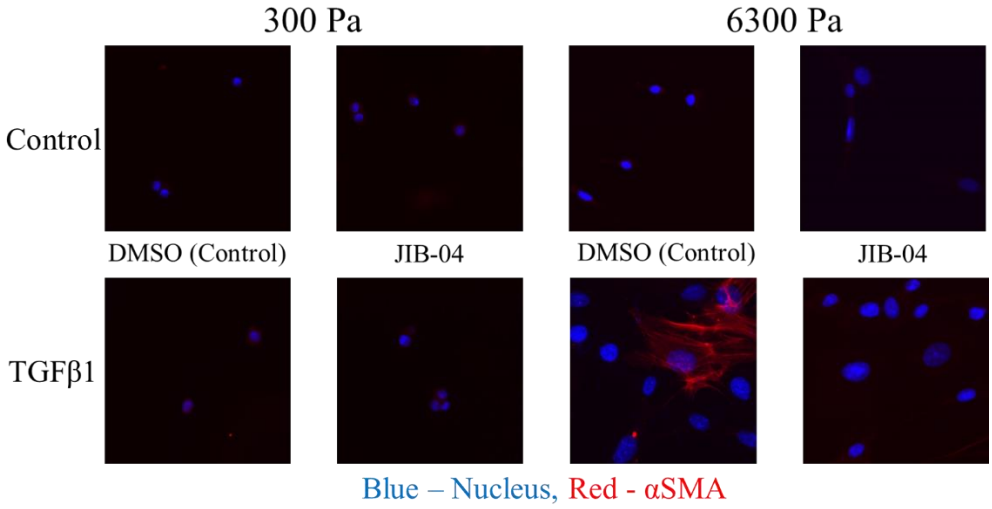


**Figure 14. Nuclear (Blue) and αSMA (Red) Immunofluorescence Staining of ± TGFβ1 and ± JIB-04 (JMJD2A Inhibitor) Treated Samples Grown on Gels of Varying Stiffness**

The fraction of cells expressing αSMA were calculated and compared across cell types and is shown in Figure 15.

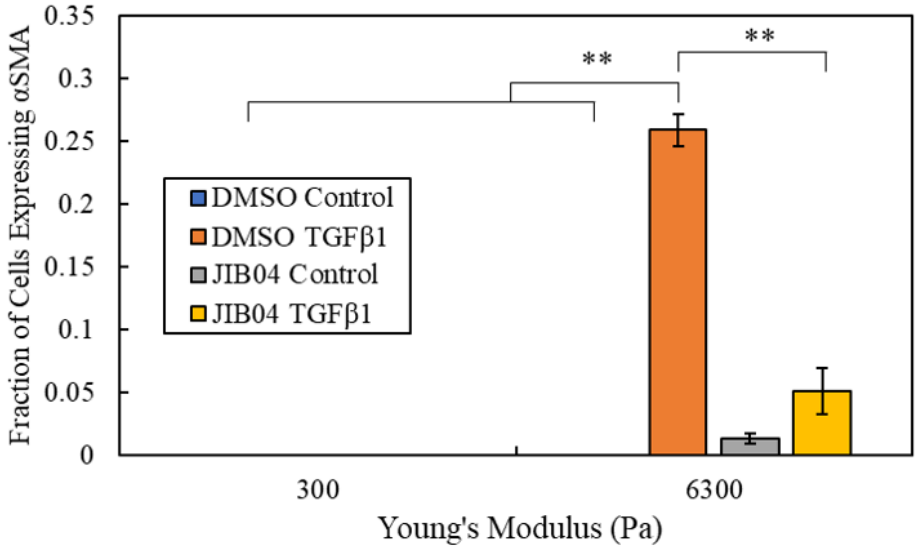


**Figure 15. Fraction of Cells Expressing αSMA for Cells Grown on Gels of Varying Stiffness with ± TGF-β1 Treatment and ± JIB-04 Inhibitor Treatment, **p<0.001**

No cells expressed αSMA on soft gels, as cells grown on soft gels should not undergo EMT after TGFβ1 treatment. On the stiff gels, the same trend seen on glass slides was observed, in which treatment with JIB-04 decreases the fraction of cells that express αSMA. It is possible the JIB-04 may have off-target effects beyond that of inhibiting JMJD2A activity; therefore, it will be important to also perform experiments where the expression of JMJD2A is depleted within the cells using siRNA to confirm whether JMJD2A is necessary for regulating aspects of TGFβ1-induced EMT.

# Chapter 4

## Conclusions and Future Work

Extracellular matrix stiffness and cell contractility play important roles in regulating the histone modifications that occur in a cell during EMT. This study showed that levels of both the acetylation of histone H4 (aH4), and the trimethylation of lysine 36 on histone H3 (H3K36Me3) increase with increasing stiffness, and that H3K36Me3 increases with TGF-β1 treatment, as shown in Figures 3 and 5. Furthermore, the studies demonstrate that treating with cell contractility inhibitors will decrease the levels of these histone marks in cells cultured on stiffer matrices as shown in Figures 6 and 7. This indicates that H3K36Me3 may be involved in the stiffness regulation of TGF-β1 mediated EMT, and that increased cell contractility may be involved in the mechanism. Additionally, levels of the histone demethylase, JMJD2A, were found to increase with increasing rigidity after TGF-β1 treatment by immunofluorescence; however, western blot data resulted in contrary results, so more experimentation needs to be performed to explain this data. Additionally, inhibition of JMJD2A resulted in a decrease in the cells expressing αSMA, as shown in Figures 14 and 16. This suggests that JMJD2A is involved in regulating αSMA, a marker of mesenchymal cells, expression, indicating that it may be important in EMT regulation.

In the future, additional experimentation should be conducted to measure JMJD2A levels in cells as a function of matrix rigidity and treatment with TGFβ1 to confirm the data presented in this thesis. Additionally, other methyltransferase and demethylase proteins should be studied, as methyltransferase proteins could play a larger role in the process. Western blots should be run to confirm the effects of inhibiting JMJD2A on αSMA, and on other epithelial and mesenchymal

markers. Finally, to see if JMJD2A is necessary for EMT, siRNA knockdown of JMJD2A can be performed to knockdown JMJD2A expression and to see if EMT will still occur.

## BIBLIOGRAPHY


1. O'Connor, J.; Gomez, E. *Clin. Trans. Med*. **2014**, *3*(23).
2. Meran, S.; Steadman, R. *International Journal of Experimental Pathology*. **2011**, *92,* 158 – 167.
3. O'Connor, J.; Gomez, *E. PLOS-ONE*. **2013**, *8*(12).
4. O'Connor, J.; Riley, P.; Nalluri, S.; Ashar, P.; Gomez, E. *J. Cell. Physiol*. **2014**, *230*, 1829-1839.
5. Ding, L.; Zhang, Z.; Shang, D.; Cheng, J.; Yuan, H.; Wu, Y.; Song, X.; Jiang, H. *J. Oral. Pathol. Med*. **2014**, *43*, 335-343.
6. Xiao, X.; Huang, C.; Zhao, C.; Gou, X.; Senavirathna, L.; Hinsdale, M.; Lloyd, P.; Liu, L. *Archives of Biochemistry and Biophysics*. **2015**, *566*, 49-57.
7. Kalluri, R.; Neilson, E. *J. Clin. Invest*. **2003**, *112*, 1776-1784.
8. Radisky, D. J. Cell Science. **2005**. *118*, 4325-4326
9. Nalluri, S.; O'Connor, J.; Gomez, E. Cytoskeleton. **2015**, *72*, 557-569.
10. Zeisberg, M.; Neilson, E. *Journal of Clinical Investigation*. **2009**, *119*(6), 1429 – 1437.
11. Lopez, J.; Kang, I.; You, W.; McDonald, D.; Weaver, V. *Integr. Biol. (Camb)*. **2011**, *3*(9), 910 – 921.
12. Acerbi, I.; Cassereau, L.; Dean, I.; Shi, Q.; Au, A.; Park, C.; Chen, Y.; Liphardt, J.; Hwang, E.; Weaver, V.; *Integr Biol (Camb)*. **2015**, *7*(10), 1120 – 1134.
13. Leight, J.; Wozniak, M., Chen, S.; Lynch, M.; Chen, C. *Molecular Biology of the Cell*. **2012**, *23*, 781-791.

14. Strahl, B.; Allis, D. *Nature*. **2000,** *403*, 41-45.

15. Lin, T.; Ponn, A.; Hu, X.; Law, B.; Lu, J. *Oncogene*. **2010**. *29*(35), 4896-4904.

16. Dong C.; Wu, Y.; Yao, J.; Wang, Y.; Yu, Y.; Rychahou, P.; Evers, B.; Zhou, B. *Journal of Clinical Investigation*. **2012**, *122*(4), 1469 – 1486.

17. Luo, X.; Zhang, C.; Zhao, W.; Liu, Z.; Liu, L.; Mu, A.; Guo, S.; Wang, N.; Zhou, H.; Zhang, T. *Cancer Letters*. **2014**, *344*, 129-137.

18. Javaid, S.; Zhang, J.; Andersen E.; Black, J.; Wittner, B.; Taijima, K.; Ting, D.; Smolen, G.; Zubrowksi, M.; Desai, R.; Maheswaran, S.; Ramaswarmy, S.; Whetstine, J.; Haber, D. *Cell Reports*. **2013**, *5*, 1679-1689.

19. McDonald, O.; Wu, H.; Timp, W.; Doi, A.; Feinberg, A. *Nature Structural and Molecular Biology*. **2011**. *18*(8), 867-874.

20. Wu, C.; Tsai, Y.; Wu, M.; Teng, S.; Wu, K. *Cell Press*. **2012**. *28*(9), 454 – 464.

# ACADEMIC VITA

**Paul Blanchard**
pmb5252@psu.edu

## EDUCATION

The Pennsylvania State University, University Park, PA
Bachelor of Science with Honors in Chemical Engineering
Minor in Biomedical Engineering

Honors Thesis: The Effect of Matrix Rigidity on Histone Modifications during Epithelial to Mesenchymal Transition
Thesis Supervisor: Dr. Esther Gomez

## PROFESSIONAL EXPERIENCE

**Undergraduate Researcher for Dr. Esther Gomez** **(**January 2015 – Present)
*Department of Chemical Engineering, The Pennsylvania State University, University Park, PA*

- Conducted experimental research studying how matrix rigidity affects the epithelial to mesenchymal transition, with application to organ fibrosis and cancer progression
- Trained two undergraduates and one graduate student in research techniques and theory
- Laboratory Skills: Mammalian cell culture, western blotting, immunofluorescence staining, fluorescence microscopy, making polyacrylamide gels, and Image J

**Chemical Engineering REU in Sustainable Energy and Materials** (June 2016-August 2016)
*Department of Chemical Engineering, University of Delaware, Newark, DE*

- Conducted computational research studying polymer nanocomposite morphology in Dr. Arthi Jayaraman's research laboratory with application to organic photovoltaic devices
- Designed and programmed coarse-grained molecular-dynamics simulations to study parameters such as polymer length, and developed python scripts to analyze the data
- Some experience with UNIX, LAMMPS modeling software, and VMD graphics software

## AWARDS

- Department of Chemical Engineering Biomolecular Fellowship (2015 and 2017)
- National Science Foundation Graduate Research Fellowship

## LEADERSHIP

**Vice President, PSU Knights of Columbus** (April 2017 – February 2017)

- Organized our first ever Christmas toy collection, along with food drives and other service

**Volunteer at Discovery Space Children's Science Museum** (March 2017 – Present)

- Helped children learn from interactive exhibits demonstrating basic science concepts

**Treasurer, Newman Catholic Society, Penn State University** (April 2015 – May 2016)

- Organized general body meetings for the Newman Catholic Association of over sixty people

**Second Degree Black Belt, Tang Soo Do** (June 2014 – Present)

- Instructed classes of over 40 students in techniques and theory of Tang Soo Do